JOURNAL OF THERMOPHYSICS AND HEAT TRANSFER
Vol. 21, No. 2, April–June 2007

Heat and Mass Transfer Characteristics for Finned Tube Heat Exchangers with Humidification

Worachest Pirompugd*
Burapha University, Saensook, Muang, Chonburi 20131, Thailand
Chi-Chuan Wang
Energy and Environment Laboratory, Industrial Technology Research Institute, 310 Taiwan, People's Republic of China
and
Somchai Wongwises†
Fluid Mechanics, Thermal Engineering and Multiphase Flow Research Laboratory (FUTURE), King Mongkut's University of Technology Thonburi, Bangmod, Bangkok 10140, Thailand.

DOI: 10.2514/1.24170

The present study proposes a new reduction method for analyzing the heat and mass transfer characteristics of wavy fin-and-tube heat exchangers under dehumidifying conditions. The analysis of the fin-and-tube heat exchangers is carried out via dividing it into many tiny segments. The proposed reduction method is applicable to the wavy fin-and-tube heat exchanger under fully wet and partially wet conditions. From the experimental results, it is found that the sensible heat transfer and mass transfer characteristics are slightly sensitive to changes in the inlet relative humidity and fin spacing. For high Reynolds numbers where partially wet condition takes place, a considerable increase of the mass transfer characteristic is encountered. The ratios of $h_{c,o}/h_{d,o}C_{p,a}$ are in the range 0.6–1.2. Correlations are proposed to describe the heat and mass transfer characteristics. These correlations can describe 99.18% of the heat transfer characteristic within 20% and 86.89% of the mass transfer characteristic within 20%. Correspondingly, 88.93% of the ratios of $h_{c,o}/h_{d,o}C_{p,a}$ are predicted by the proposed correlation within 20%.

Nomenclature

A_f = surface area of the fin
$A_{p,\text{in}}$ = inside surface area of the tube
$A_{p,\text{out}}$ = outside surface area of the tube
A_{tot} = total surface area that is the summation of A_f and $A_{p,\text{out}}$
A_{wet} = wet fin surface area
b'_p = slope of the saturated moist air enthalpy curved between the mean inside and outside tube surface temperatures
b'_r = slope of the saturated moist air enthalpy curved between the mean water temperature and the mean inside tube surface temperature
b'_{wff} = slope of the saturated moist air enthalpy curved at the mean water film temperature of the fin surface
$b'_{\text{wf},p,\text{out}}$ = slope of the saturated moist air enthalpy curved at the mean water film temperature of the outside tube surface
$C_{p,a}$ = moist air specific heat at the constant pressure
$C_{p,w}$ = water specific heat at the constant pressure
D_c = collar diameter
$D_{p,\text{in}}$ = inside tube diameter
$D_{p,\text{out}}$ = outside tube diameter (include very tiny collar) that is equal to the collar diameter
F = correction factor
F_p = fin pitch
f_{in} = water-side friction factor
$G_{a,\text{max}}$ = moist air maximum mass velocity based on the minimum flow area
$h_{c,\text{in}}$ = water-side convection heat transfer coefficient
$h_{c,\text{out}}$ = moist air-side convection heat transfer coefficient
$h_{c,\text{wf},f}$ = heat transfer coefficient for the heat transfer between the moist air and fin surface
$h_{c,\text{wf},p,\text{out}}$ = heat transfer coefficient for the heat transfer between the moist air and outside tube surface
$h_{d,\text{out}}$ = moist air-side convection mass transfer coefficient
I_0 = modified Bessel function solution of the first kind, order 0.
I_1 = modified Bessel function solution of the first kind, order 1.
i_a = moist air enthalpy
$i_{a,\text{in}}$ = inlet moist air enthalpy
$i_{a,m}$ = mean moist air enthalpy
$i_{a,m,\text{cf}}$ = mean moist air enthalpy for the counterflow configuration
$i_{a,\text{out}}$ = outlet moist air enthalpy
$i_{r,f,m}$ = mean saturated moist air enthalpy at the mean fin surface temperature
$i_{r,f,m,\text{cf}}$ = mean saturated moist air enthalpy at the mean fin surface temperature for the counterflow configuration
$i_{r,\text{in}}$ = saturated moist air enthalpy at the inlet water temperature
$i_{r,m,\text{cf}}$ = mean saturated moist air enthalpy at the mean water temperature for the counterflow configuration
$i_{r,\text{out}}$ = saturated moist air enthalpy at the outlet water temperature
$i_{r,p,\text{in},m,\text{cf}}$ = mean saturated moist air enthalpy at the mean inside tube surface temperature for the counterflow configuration
$i_{r,p,\text{out},m}$ = mean saturated moist air enthalpy at the mean outside tube surface temperature

Received 23 March 2006; revision received 3 November 2006; accepted for publication 30 November 2006.

*Department of Mechanical Engineering, Faculty of Engineering.
†Corresponding Author, Department of Mechanical Engineering; somchai.won@kmutt.ac.th.

$i_{r,p,\text{out},m,\text{cf}}$ = mean saturated moist air enthalpy at the mean outside tube surface temperature for the counterflow configuration
i_{wf} = saturated moist air enthalpy at the water film temperature
$i_{w,g}$ = specific enthalpy of the saturated water vapor
j_h = Colburn heat transfer group or Chilton–Colburn j-factor for the heat transfer
j_m = Colburn mass transfer group or Chilton–Colburn j-factor for the mass transfer
K_0 = modified Bessel function solution of the second kind, order 0
K_1 = modified Bessel function solution of the second kind, order 1
k_f = thermal conductivity of the fin
k_p = thermal conductivity of the tube
k_w = thermal conductivity of the water
k_{wf} = thermal conductivity of the water film
L_p = tube length
$\dot{m}_a$ = moist air mass flow rate
$\dot{m}_w$ = water mass flow rate
N = number of tube row
P_d = wave height
P_l = longitudinal tube pitch
Pr_{in} = water-side Prandtl number
Pr_{out} = moist air-side Prandtl number
P_t = transverse tube pitch
$\dot{Q}_a$ = moist air-side heat transfer rate
$\dot{Q}_{\text{avg}}$ = average heat transfer rate between the moist air and water sides
$\dot{Q}_w$ = water-side heat transfer rate
$\dot{Q}_{\text{wet}}$ = heat transfer rate for a fully wet segment
R = ratio of the convection heat transfer characteristic to the convection mass transfer characteristic for the simultaneous convection heat and mass transfer
Re_{D_c} = moist air-side Reynolds number based on the collar diameter
Re_{in} = water-side Reynolds number
RH = inlet relative humidity of the moist air
r_i = inside fin radius for the equivalent circular fin that equal the outside tube (include collar) radius
r_o = outside fin radius for the equivalent circular fin
Sc_{out} = moist air-side Schmidt number
S_p = fin spacing
T_a = moist air temperature
$T_{a,\text{in}}$ = inlet moist air temperature
$T_{a,m,\text{cf}}$ = mean moist air temperature for the counterflow configuration
$T_{a,\text{out}}$ = outlet moist air temperature
T_{dp} = dew point temperature of the moist air
$T_{f,b}$ = fin base temperature
$T_{f,t}$ = fin tip temperature
$T_{f,m,\text{cf}}$ = mean fin temperature
$T_{p,\text{in},m,\text{cf}}$ = mean inside tube surface temperature for the counterflow configuration
$T_{p,\text{out},m,\text{cf}}$ = mean outside tube surface temperature for the counterflow configuration
$T_{r,m,\text{cf}}$ = mean water temperature for the counterflow configuration
T_w = water temperature
$T_{w,\text{in}}$ = inlet water temperature
$T_{w,\text{out}}$ = outlet water temperature
$T_{w,m,\text{cf}}$ = mean water temperature for the counterflow configuration
t = fin thickness
U_i = overall heat transfer coefficient based on the mean enthalpy difference
U_T = overall heat transfer coefficient based on the mean temperature difference
W_a = moist air humidity ratio
$W_{a,\text{in}}$ = inlet moist air humidity ratio
$W_{a,m}$ = mean moist air humidity ratio
$W_{a,\text{out}}$ = outlet moist air humidity ratio
$W_{r,f,m}$ = mean saturated moist air humidity ratio at the mean fin surface temperature
$W_{r,p,\text{out},m}$ = mean saturated moist air humidity ratio at the mean outside tube surface temperature
W_{wf} = saturated moist air humidity ratio at the water film temperature
X_f = projected fin length
y_{wf} = thickness of the water film
$\Delta i_{m,\text{cf}}$ = logarithmic mean enthalpy difference across the heat exchanger for the counterflow double-pipe configuration with the hot and cold fluid enthalpies
ΔP = pressure difference
$\Delta T_{m,\text{cf}}$ = logarithmic mean temperature difference across the heat exchanger for the counterflow double-pipe configuration with the hot and cold fluid temperatures
$\eta_{f,\text{dry}}$ = dry fin efficiency
$\eta_{f,\text{wet}}$ = wet fin efficiency

I. Introduction

FIN-AND-TUBE heat exchangers are a basic type of heat exchanger employed in many industrial applications such as air conditioning, refrigeration, and other thermal processes. In application, the dominated thermal resistance on the air side of the heat exchanger normally limits the heat transfer rate. One way to enhance the heat transfer on the air side of the heat exchanger is to modify the fin geometry. Almost every residential air-conditioning system and refrigeration system contains at least two heat exchangers, so called the evaporator and the condenser. In the evaporators, when the surface temperature of the heat exchanger is below the dew point temperature of the incoming air, a portion of the water vapor in the humid air system is condensed on the surface. As a consequence, simultaneous heat and mass transfer occurs along the fin surfaces. In general, the complexity of the moist airflow pattern across the fin-and-tube heat exchangers under dehumidifying conditions makes theoretical simulations very difficult. Accordingly, it is necessary to resort to experimentation.

For a better improvement of the overall performance of fin-and-tube heat exchangers, the fin surface can be in the form of enhanced surfaces such as wavy, louver, and slit. The wavy fin surface is one of the most popular surfaces, because it can lengthen the flow path and disturb the airflow without considerable increase of pressure drop. The air-side performance of wavy fin-and-tube heat exchangers has been studied by many researchers (Beecher and Fagan [1], Yan and Sheen [2], Wang et al. [3–6], Lin et al. [7], Pirompugd et al. [8]). Even though many efforts have been devoted to the study of wet coils, the available literature on dehumidifying heat exchangers still offers limited information to assist the designer in sizing and rating a fin-and-tube heat exchanger. This can be made clear from the reported data, which mainly focused on the study of the sensible heat transfer characteristics; little attention was paid to the mass transfer characteristics. Moreover, the fin surfaces may be wet or dry depending on the difference between the dew point temperature and surface temperature. Notice that if the dew point temperature of moist air is lower than the outside tube (including collar) temperature, there is only sensible heat transfer and it is termed as the fully dry condition. However, if the dew point temperature of moist air is higher than the fin tip temperature, sensible and latent heat transfer occur at the same time for all fin surfaces. This condition is regarded as the fully wet condition. It is found that the available literature concerning the heat transfer characteristic are either related to the fully dry condition or to completely wet surface. In that regard, it is the objective of this study to provide a detailed method for analyzing the partially wet condition.

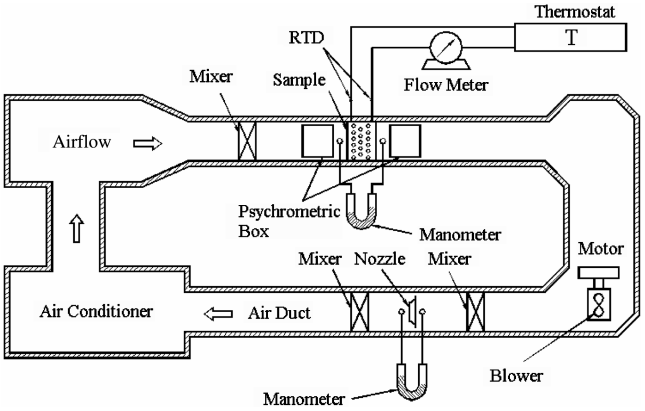

Fig. 1 Schematic diagram of experimental apparatus.

II. Experimental Apparatus

Figure 1 shows the schematic diagram of the experimental apparatus. It consists of a closed-loop wind tunnel in which air is circulated by a centrifugal fan (7.46 kW, 10 hp) varying the air velocity with an inverter. The air duct is made from galvanized sheet steel and has an 850 × 550 mm cross section. To obtain a uniform flow into the tested channel, air is forced through a mixer before entering the test section. The airflow is measured by multiple nozzles based on the ASHRAE 41.2 standard [9]. A differential pressure transducer is used to measure the pressure difference across the nozzles. The air temperatures at the inlet and exit zones across the sample heat exchangers are measured by two psychrometric boxes based on the ASHRAE 41.1 standard [10]. The dry-bulb and wet-bulb temperatures of the inlet air are controlled by an air ventilator that can provide a cooling capacity of up to 21.12 kW (6RT).

The working fluid in the tube side of the heat exchanger is chilled water. A thermostatically controlled reservoir provides cold water at selected temperatures. The temperature differences on the water side are measured by two precalibrated resistance temperature detectors (Pt-100Ω). The water volumetric flow rate is measured by a magnetic flow meter with a precision of ±0.001 L/s. All the temperature measuring probes are resistance temperature devices, with a calibrated accuracy of ±0.05°C. In the experiments, only the data that satisfy the ASHRAE 33 Standard [11] requirements (the energy balance condition, $|\dot{Q}_a - \dot{Q}_w|/\dot{Q}_{\text{avg}}$, is less than 0.05) are considered in the final analysis. A total of 17 wavy fin-and-tube heat exchangers, having various geometric parameters, are tested in this study. The details of test samples are shown in Table 1. The accuracies of the measurement sensors and the uncertainties in derived experimental values following the single-sample analysis proposed by Moffat [12] are given in Table 2. The geometrical parameters can be seen in Fig. 2. The geometric details of the tested wavy fins are shown in Fig. 3. The test fin-and-tube heat exchangers are tension wrapped having a "L"-type fin collar. The test conditions approximate those encountered with typical fan coils and evaporators of air-conditioning applications.

The test conditions of the inlet-air are as follows:
Dry-bulb temperature of the air: 27 ± 0.5 °C
Inlet relative humidity for the incoming air: 50 and 90%
Inlet air velocity: from 0.3 to 4.5 m/s
Inlet water temperature: 7 ± 0.5 °C
Water velocity inside the tube: 1.5–1.7 m/s

Table 2 Summary of estimated uncertainties

Primary measurements		Derived quantities		
Parameter	Uncertainty	Parameter	Uncertainty $Re_{D_c} = 400$	Uncertainty $Re_{D_c} = 5000$
$\dot{m}_a$	0.3–1%	Re_{D_c}	±1.0%	±0.57%
$\dot{m}_w$	0.5%	Re_{Di}	±0.73%	±0.73%
ΔP	0.5%	$\dot{Q}_w$	±3.95%	±1.22%
T_w	0.05°C	$\dot{Q}_a$	±5.5%	±2.4%
T_a	0.1°C	j_h, j_m	±11.4%	±5.9%

III. Mathematical Model

The total heat transfer rate used in the calculation is the average of $\dot{Q}_a$ and $\dot{Q}_w$, namely,

$$\dot{Q}_a = \dot{m}_a(i_{a,\text{in}} - i_{a,\text{out}}) \tag{1}$$

$$\dot{Q}_w = \dot{m}_w C_{p,w}(T_{w,\text{out}} - T_{w,\text{in}}) \tag{2}$$

$$\dot{Q}_{\text{avg}} = \frac{\dot{Q}_a + \dot{Q}_w}{2} \tag{3}$$

In this study, a new method, namely, the "fully wet and fully dry tiny circular fin method" is presented to evaluate the heat and mass transfer performances of wavy fin-and-tube heat exchangers. The analysis is done by dividing the wavy fin-and-tube heat exchangers into many tiny segments (number of tube row× number of tube pass per row × number of fin) as shown in Fig. 4. The equivalent circular area method as shown in Fig. 5 is adopted for calculation of the fin efficiency. Two heat transfer modes are identified. The first one is the fully dry condition, in which the dew point temperature of the moist air is lower than the tube surface (including collar) temperature (as shown in Fig. 6a). As a result, only sensible heat transfer occurs on the whole area of this tiny segment. The other case is the fully wet condition, in which the dew point temperature of moist air is higher than the fin

Table 1 Geometric dimensions of the sample wavy fin-and-tube heat exchangers

No.	F_p, mm	S_p, mm	t, mm	D_c, mm	P_t, mm	P_l, mm	P_d, mm	X_f, mm	N
1	1.60	1.48	0.12	10.38	25.4	19.05	1.18	4.7625	1
2	2.82	2.70	0.12	10.38	25.4	19.05	1.18	4.7625	1
3	2.92	2.80	0.12	8.62	25.4	19.05	1.58	4.7625	1
4	3.54	3.42	0.12	8.62	25.4	19.05	1.58	4.7625	1
5	3.63	3.51	0.12	8.62	25.4	25.40	1.68	6.3500	1
6	1.69	1.57	0.12	8.62	25.4	19.05	1.18	4.7625	2
7	1.71	1.59	0.12	8.62	25.4	19.05	1.58	4.7625	2
8	3.12	3.00	0.12	8.62	25.4	19.05	1.58	4.7625	2
9	3.17	3.05	0.12	8.62	25.4	19.05	1.18	4.7625	2
10	1.64	1.52	0.12	8.62	25.4	19.05	1.58	4.7625	4
11	1.70	1.58	0.12	8.62	25.4	19.05	1.18	4.7625	4
12	3.07	2.95	0.12	8.62	25.4	19.05	1.58	4.7625	4
13	3.14	3.02	0.12	8.62	25.4	19.05	1.18	4.7625	4
14	1.57	1.45	0.12	10.38	25.4	19.05	1.18	4.7625	6
15	1.65	1.53	0.12	8.62	25.4	19.05	1.58	4.7625	6
16	2.82	2.70	0.12	10.38	25.4	19.05	1.18	4.7625	6
17	3.06	2.94	0.12	8.62	25.4	19.05	1.58	4.7625	6

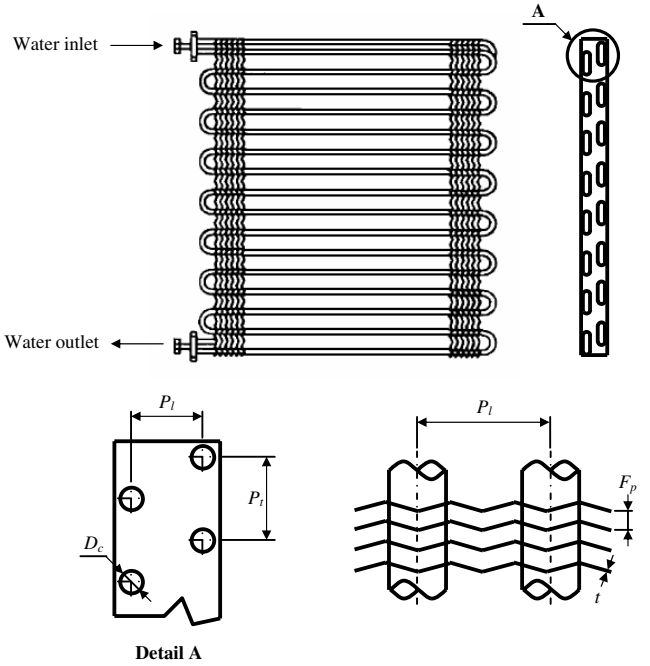

Fig. 2 Geometric detail of the wavy fin-and-tube heat exchanger.

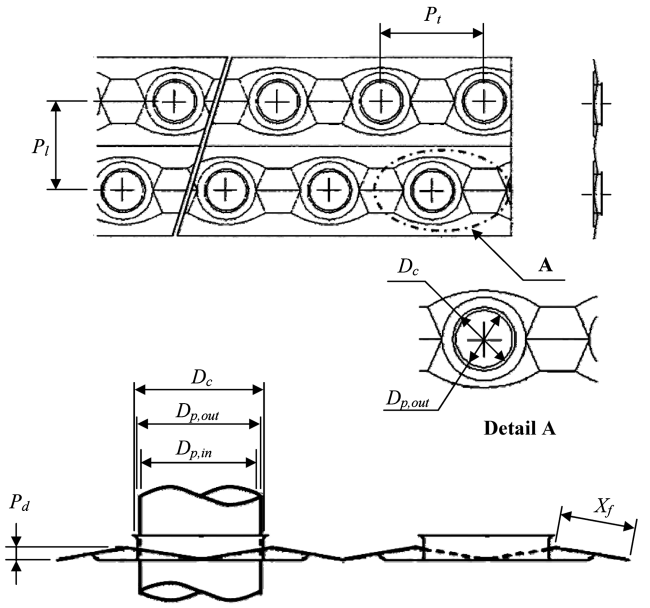

Fig. 3 Geometric detail of the herringbone wavy fin.

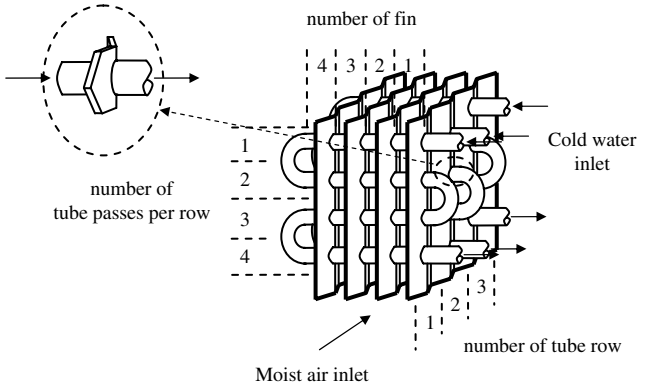

Fig. 4 Schematic of the wavy fin-and-tube heat exchanger used for data reduction.

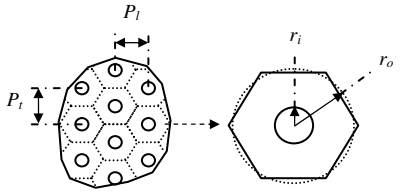

Fig. 5 Equivalent circular area method.

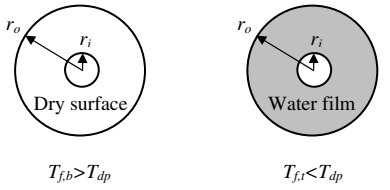

a) Fully dry condition b) Fully wet condition

Fig. 6 Circular fin in fully dry and fully wet conditions.

tip temperature (as shown in Fig. 6b). Both sensible and latent heat transfer take place along the area of each tiny segment.

A. Tiny Circular Fin Under Fully Dry Condition

The new method, namely, fully wet and fully dry tiny circular fin method for the wavy fin-and-tube heat exchangers, is based on the method of Threlkeld [13]. For fully dry condition, the overall heat transfer coefficient U_T based on the temperature difference is given as follows:

$$\dot{Q}_{\text{dry}} = U_T A_{\text{tot}} \Delta T_{m,\text{cf}} F \tag{4}$$

The term of $\Delta T_{m,\text{cf}}$ can be shown as

$$\Delta T_{m,\text{cf}} = T_{a,m,\text{cf}} - T_{w,m,\text{cf}} \tag{5}$$

According to Bump [14], for the counterflow configuration, the mean temperature difference is

$$T_{a,m,\text{cf}} = T_{a,\text{in}} + \frac{T_{a,\text{in}} - T_{a,\text{out}}}{\ell n[(T_{a,\text{in}} - T_{w,\text{out}})/(T_{a,\text{out}} - T_{w,\text{in}})]} - \frac{(T_{a,\text{in}} - T_{a,\text{out}})(T_{a,\text{in}} - T_{w,\text{out}})}{(T_{a,\text{in}} - T_{w,\text{out}}) - (T_{a,\text{out}} - T_{w,\text{in}})} \tag{6}$$

$$T_{w,m,\text{cf}} = T_{w,\text{out}} + \frac{T_{w,\text{out}} - T_{w,\text{in}}}{\ell n[(T_{a,\text{in}} - T_{w,\text{out}})/(T_{a,\text{out}} - T_{w,\text{in}})]} - \frac{(T_{w,\text{out}} - T_{w,\text{in}})(T_{a,\text{in}} - T_{w,\text{out}})}{(T_{a,\text{in}} - T_{r,\text{out}}) - (T_{a,\text{out}} - T_{w,\text{in}})} \tag{7}$$

In the analysis, the water temperature in the tiny tube is almost constant. Then, F can be approximated to unity. The overall heat transfer coefficient is showed as follows:

$$\frac{1}{U_T} = \frac{A_{\text{tot}}}{h_{c,\text{in}} A_{p,\text{in}}} + \frac{A_{\text{tot}}\, \ell n(D_{p,\text{out}}/D_{p,\text{in}})}{2\pi k_p L_p} + \frac{1}{h_{c,\text{out}} A_{p,\text{out}}/A_{\text{tot}} + h_{c,\text{out}} A_f \eta_{f,\text{dry}}/A_{\text{tot}}} \tag{8}$$

The water-side heat transfer coefficient obtained from the Gnielinski semiempirical correlation [15] is

$$h_{c,\text{in}} = \frac{(f_{\text{in}}/2)(Re_{\text{in}} - 1000)Pr_{\text{in}}}{1.07 + 12.7\sqrt{f_{\text{in}}/2}(Pr_{\text{in}}^{2/3} - 1)} \frac{k_w}{D_{p,\text{in}}} \tag{9}$$

and the friction factor f_{in} is

$$f_{\text{in}} = \frac{1}{(1.58\, \ell n\, Re_{\text{in}} - 3.28)^2} \tag{10}$$

The Reynolds number used in Eqs. (9) and (10) is based on the inside tube diameter. The dry fin efficiency $\eta_{f,\mathrm{dry}}$ is based on the temperature difference shown as

$$\eta_{f,\mathrm{dry}} = \frac{T_{a,m,\mathrm{cf}} - T_{f,m,\mathrm{cf}}}{T_{a,m,\mathrm{cf}} - T_{p,\mathrm{out},m,\mathrm{cf}}} \tag{11}$$

Kern and Kraus [16] determined the dry fin efficiency for a circular fin as follows:

$$\eta_{f,\mathrm{dry}} = \frac{2r_i}{M_m(r_o^2 - r_i^2)}\left[\frac{K_1(M_m r_i)I_1(M_m r_o) - K_1(M_m r_o)I_1(M_m r_i)}{K_1(M_m r_o)I_0(M_m r_i) + K_0(M_m r_i)I_1(M_m r_o)}\right] \tag{12}$$

where

$$M_m = \sqrt{\frac{2h_{c,\mathrm{out}}}{k_f t}} \tag{13}$$

An algorithm for solving the heat transfer characteristic for the fully dry condition is given as follows:

1. Based on the information, calculate the average heat transfer rate $\dot{Q}_{\mathrm{avg}}$ using Eq. (3).
2. Assume a $h_{c,\mathrm{out}}$ for all elements.
3. Calculate the heat transfer characteristic for each segment with the following procedures:
   3.1 Calculate the tube-side heat transfer coefficient of h_i using Eq. (9).
   3.2 Assume an outlet air enthalpy of the calculated segment.
   3.3 Calculate $T_{a,m,\mathrm{cf}}$ and $T_{w,m,\mathrm{cf}}$ by Eqs. (6) and (7).
   3.4 Calculate $1/h_{c,\mathrm{in}}A_{p,\mathrm{in}}$ and $[\ell_n(D_{p,\mathrm{out}}/D_{p,\mathrm{in}})/2\pi k_p L_p]$.
   3.5 Calculate $\eta_{f,\mathrm{dry}}$ using Eq. (12).
   3.6 Calculate U_T from Eq. (8).
   3.7 Calculate $\dot{Q}_{\mathrm{dry}}$ of this segment.
   3.8 Calculate the outlet air enthalpy and the outlet water temperature from $\dot{Q}_{\mathrm{dry}}$ obtained in step 3.7.
   3.9 If the outlet air enthalpy obtained in step 3.8 is not equal to the assumed value in step 3.2, the calculation steps 3.3–3.8 will be repeated.
4. If the summation of the heat transfer rate $\dot{Q}$ for all elements is not equal to $\dot{Q}_{\mathrm{avg}}$, $h_{c,\mathrm{out}}$ will be assumed with a new value and the calculation step 3 will be repeated until the summation of the heat transfer rate $\dot{Q}$ for all elements is equal to $\dot{Q}_{\mathrm{avg}}$.

B. Tiny Circular Fin Under Fully Wet Condition

1. Heat Transfer

The overall heat transfer coefficient U_i is based on the enthalpy potential and is given as follows:

$$\dot{Q}_{\mathrm{wet}} = U_i A_{\mathrm{tot}} \Delta i_{m,\mathrm{cf}} F \tag{14}$$

The term of $\Delta i_{m,\mathrm{cf}}$ can be shown as

$$\Delta i_{m,\mathrm{cf}} = i_{a,m,\mathrm{cf}} - i_{r,m,\mathrm{cf}} \tag{15}$$

Bump [14] and Myers [17] determined the mean enthalpy for the counterflow configuration as follows:

$$i_{a,m,\mathrm{cf}} = i_{a,\mathrm{in}} + \frac{i_{a,\mathrm{in}} - i_{a,\mathrm{out}}}{\ell_n[(i_{a,\mathrm{in}} - i_{r,\mathrm{out}})/(i_{a,\mathrm{out}} - i_{r,\mathrm{in}})]} - \frac{(i_{a,\mathrm{in}} - i_{a,\mathrm{out}})(i_{a,\mathrm{in}} - i_{r,\mathrm{out}})}{(i_{a,\mathrm{in}} - i_{r,\mathrm{out}}) - (i_{a,\mathrm{out}} - i_{r,\mathrm{in}})} \tag{16}$$

$$i_{r,m,\mathrm{cf}} = i_{r,\mathrm{out}} + \frac{i_{r,\mathrm{out}} - i_{r,\mathrm{in}}}{\ell_n[(i_{a,\mathrm{in}} - i_{r,\mathrm{out}})/(i_{a,\mathrm{out}} - i_{r,\mathrm{in}})]} - \frac{(i_{r,\mathrm{out}} - i_{r,\mathrm{in}})(i_{a,\mathrm{in}} - i_{r,\mathrm{out}})}{(i_{a,\mathrm{in}} - i_{r,\mathrm{out}}) - (i_{a,\mathrm{out}} - i_{r,\mathrm{in}})} \tag{17}$$

For a tiny segment, $i_{r,\mathrm{in}}$ is nearly equal to $i_{r,\mathrm{out}}$ and then, F can be approximated to unity. The overall heat transfer coefficient is related to the individual heat transfer resistances (Myers [17]) as follows:

$$\frac{1}{U_i} = \frac{b'_r A_{\mathrm{tot}}}{h_{c,\mathrm{in}}A_{p,\mathrm{in}}} + \frac{b'_p A_{\mathrm{tot}}\,\ell_n(D_{p,\mathrm{out}}/D_{p,\mathrm{in}})}{2\pi k_p L_p} + \frac{1}{h_{c,\mathrm{wf},p,\mathrm{out}}A_{p,\mathrm{out}}/b'_{\mathrm{wf},p,\mathrm{out}}A_{\mathrm{tot}} + h_{c,\mathrm{wf},f}A_f\eta_{f,\mathrm{wet}}/b'_{\mathrm{wf},f}A_{\mathrm{tot}}} \tag{18}$$

The water film is very thin, then

$$h_{c,\mathrm{wf},f} = \frac{1}{C_{p,a}/b'_{\mathrm{wf},f}h_{c,\mathrm{out}} + y_{\mathrm{wf}}/k_{\mathrm{wf}}} \tag{19}$$

$$h_{c,\mathrm{wf},p,\mathrm{out}} = \frac{1}{C_{p,a}/b'_{\mathrm{wf},p,\mathrm{out}}h_{c,\mathrm{out}} + y_{\mathrm{wf}}/k_{\mathrm{wf}}} \tag{20}$$

y_{wf} in Eqs. (9) and (10) are the thickness of the water film. A constant of 0.013 cm was proposed by Myers [17]. In practice, $y_{\mathrm{wf}}/k_{\mathrm{wf}}$ accounts for only 0.5–5 percent compared to $C_{p,a}/b'_{\mathrm{wf},f}h_{c,\mathrm{out}}$ and $C_{p,a}/b'_{\mathrm{wf},p,\mathrm{out}}h_{c,\mathrm{out}}$, and has often been neglected by previous investigators. As a result, this term is not included in the final analysis. The water-side heat transfer coefficient can be calculated by Gnielinski [15] as shown in Eq. (9). In Eq. (18) b'_p, b'_r, $b'_{\mathrm{wf},f}$, and $b'_{\mathrm{wf},p,\mathrm{out}}$ those are the ratios of enthalpy to temperature must be evaluated. The quantities b'_p and b'_r can be calculated as

$$b'_r = \frac{i_{r,p,\mathrm{in},m,\mathrm{cf}} - i_{r,m,\mathrm{cf}}}{T_{p,\mathrm{in},m,\mathrm{cf}} - T_{r,m,\mathrm{cf}}} \tag{21}$$

$$b'_p = \frac{i_{r,p,\mathrm{out},m,\mathrm{cf}} - i_{r,p,\mathrm{in},m,\mathrm{cf}}}{T_{p,\mathrm{out},m,\mathrm{cf}} - T_{p,\mathrm{in},m,\mathrm{cf}}} \tag{22}$$

The values of $b'_{\mathrm{wf},f}$ and $b'_{\mathrm{wf},p,\mathrm{out}}$ are the slope of the saturated moist air enthalpy curved at the mean water film temperatures of the fin and outside tube surfaces, respectively. Without loss of generality, $b'_{\mathrm{wf},f}$ and $b'_{\mathrm{wf},p,\mathrm{out}}$ can be approximated by the slope of the saturated moist air enthalpy curved at the mean fin surface temperature $T_{f,m,\mathrm{cf}}$ and the mean outside tube surface temperature $T_{p,\mathrm{out},m,\mathrm{cf}}$ (Wang et al. [18]). However, the evaluation of $b'_{\mathrm{wf},f}$ is derived by the trial and error procedure that is depended on the wet fin efficiency. Then, the wet fin efficiency $\eta_{f,\mathrm{wet}}$ is based on the enthalpy difference proposed by Threlkeld [13]:

$$\eta_{f,\mathrm{wet}} = \frac{i_{a,m,\mathrm{cf}} - i_{r,f,m,\mathrm{cf}}}{i_{a,m,\mathrm{cf}} - i_{r,p,\mathrm{out},m,\mathrm{cf}}} \tag{23}$$

The use of the enthalpy potential equation greatly simplifies the fin efficiency calculation as illustrated by Kandlikar [19]. However, the original formulation of the wet fin efficiency by Threlkeld [13] was for straight-fin configuration. For a circular fin, the wet fin efficiency is given by Wang et al. [18] as follows:

$$\eta_{f,\mathrm{wet}} = \frac{2r_i}{M_T\left(r_o^2 - r_i^2\right)}\left[\frac{K_1(M_T r_i)I_1(M_T r_o) - K_1(M_T r_o)I_1(M_T r_i)}{K_1(M_T r_o)I_0(M_T r_i) + K_0(M_T r_i)I_1(M_T r_o)}\right] \tag{24}$$

where

$$M_T = \sqrt{\frac{2h_{c,\mathrm{wf},f}}{k_f t}} \tag{25}$$

The evaluation of $b'_{\mathrm{wf},f}$ requires a trial and error procedure. For the trial and error procedure, $i_{r,f,m,\mathrm{cf}}$ must be calculated using the following equation:

$$i_{r,f,m,\mathrm{cf}} = i_{a,m,\mathrm{cf}} - \eta_{f,\mathrm{wet}}\left(1 - U_i A_{\mathrm{tot}}\left[\frac{b'_r}{h_{c,\mathrm{in}}A_{p,\mathrm{in}}} + \frac{b'_p\,\ell n(D_{p,\mathrm{out}}/D_{p,\mathrm{in}})}{2\pi k_p L_p}\right]\right)\Delta i_{m,\mathrm{cf}} \tag{26}$$

An algorithm for solving the heat transfer characteristic for the fully wet condition is given as follows:

1. Based on the information, calculate the average heat transfer rate $\dot{Q}_{\mathrm{avg}}$ using Eq. (3).
2. Assume a $h_{c,\mathrm{out}}$ for all elements.
3. Calculate the heat transfer characteristic for each segment with the following procedures:
   3.1 Calculate the water-side heat transfer coefficient of $h_{c,\mathrm{in}}$ using Eq. (9).
   3.2 Assume an outlet moist air enthalpy of the calculated segment.
   3.3 Calculate $i_{a,m,\mathrm{cf}}$ and $i_{r,m,\mathrm{cf}}$ by Eqs. (16) and (17).
   3.4 Assume $T_{p,\mathrm{in},m,\mathrm{cf}}$ and $T_{p,\mathrm{out},m,\mathrm{cf}}$.
   3.5 Calculate $b'_r/h_{c,\mathrm{in}}A_{p,\mathrm{in}}$ and $b'_p\,\ell n(D_{p,\mathrm{out}}/D_{p,\mathrm{in}})/2\pi k_p L_p$.
   3.6 Assume a $T_{f,m,\mathrm{cf}}$.
   3.7 Calculate $\eta_{f,\mathrm{wet}}$ using Eq. (24).
   3.8 Calculate U_i from Eq. (18).
   3.9 Calculate $i_{r,f,m,\mathrm{cf}}$ by Eq. (26).
   3.10 Calculate $T_{f,m,\mathrm{cf}}$ from $i_{r,f,m,\mathrm{cf}}$.
   3.11 If $T_{f,m,\mathrm{cf}}$ calculated in step 3.10 is not equal to the assumed value in step 3.6, the calculation steps 3.7–3.10 will be repeated until these two values are equal to each other.
   3.12 Calculate the heat transfer rate $\dot{Q}$ of this segment.
   3.13 Calculate $T_{p,\mathrm{in},m,\mathrm{cf}}$ and $T_{p,\mathrm{out},m,\mathrm{cf}}$ from the water-side convection heat transfer and the conduction heat transfer of tube.
   3.14 If $T_{p,\mathrm{in},m,\mathrm{cf}}$ and $T_{p,\mathrm{out},m,\mathrm{cf}}$ calculated in step 3.13 are not equal to the assumed value in step 3.4, the calculation steps 3.5–3.13 will be repeated until these two values are equal to each other.
   3.15 Calculate the outlet moist air enthalpy by Eq. (1) and the outlet water temperature by Eq. (2).
   3.16 If the outlet moist air enthalpy calculated in step 3.15 is not equal to the assumed value in step 3.2, the calculation steps 3.3–3.15 will be repeated until these two values are equal.
4. If the summation of the heat transfer rate $\dot{Q}$ for all elements is not equal to $\dot{Q}_{\mathrm{avg}}$, $h_{c,\mathrm{out}}$ will be assumed with a new value and the calculation step 3 will be repeated until the summation of the heat transfer rate $\dot{Q}$ for all elements is equal to $\dot{Q}_{\mathrm{avg}}$.

2. Mass Transfer

For the fully wet condition, the cooling and dehumidifying of the moist air by a cold surface involves the simultaneous heat and mass transfer and can be described by the process line equation (SI unit) from Threlkeld [13].

$$\frac{\mathrm{d}i_a}{\mathrm{d}W_a} = R\frac{(i_a - i_{wf})}{(W_a - W_{wf})} + (i_{w,g} - 2501R) \tag{27}$$

and

$$R = \frac{h_{c,\mathrm{out}}}{h_{d,\mathrm{out}}C_{p,a}} \tag{28}$$

However, for the present fin-and-tube heat exchanger, Eq. (27) did not directly describe the dehumidification process. This is because the saturated moist air enthalpy i_{wf} at the mean water film temperature on the fin surface is different from that at the outside tube surface. In this regard, a modification of the process line chart corresponding to the fin-and-tube heat exchangers is made. From the energy balance of the dehumidification, the rate equation can be arrived at the following expression:

$$\dot{m}_a\,\mathrm{d}i_a = \frac{h_{c,\mathrm{out}}}{C_{p,a}}\,\mathrm{d}A_{p,\mathrm{out}}(i_{a,m} - i_{r,p,\mathrm{out},m}) + \frac{h_{c,\mathrm{out}}}{C_{p,a}}\,\mathrm{d}A_f(i_{a,m} - i_{r,f,m}) \tag{29}$$

Note that the first term on the right-hand side denotes the heat transfer of the outside tube, whereas the second term is the heat transfer for the fin part. Conservation of the water condensate gives

$$\dot{m}_a\,\mathrm{d}W_a = h_{d,\mathrm{out}}\,\mathrm{d}A_{p,\mathrm{out}}(W_{a,m} - W_{r,p,\mathrm{out},m}) + h_{d,\mathrm{out}}\,\mathrm{d}A_f(W_{a,m} - W_{r,f,m}) \tag{30}$$

Dividing the equation of the heat transfer rate [Eq. (29)] by the equation of the mass transfer rate [Eq. (30)] yields

$$\frac{\mathrm{d}i_a}{\mathrm{d}W_a} = \frac{R(i_{a,m} - i_{r,p,\mathrm{out},m}) + R(\varepsilon - 1)(i_{a,m} - i_{r,f,m})}{(W_{a,m} - W_{r,p,\mathrm{out},m}) + (\varepsilon - 1)(W_{a,m} - W_{r,f,m})} \tag{31}$$

where

$$\varepsilon = \frac{A_{\mathrm{tot}}}{A_{p,\mathrm{out}}} \tag{32}$$

By assuming a value of the ratio of heat transfer to mass transfer, R, and by integrating Eq. (31) with an iterative algorithm, the moist air-side convective mass transfer performance can be obtained. Analogous procedures for obtaining the mass transfer characteristic are given as follows:

1. Obtain $W_{r,p,\mathrm{out},m}$ and $W_{r,f,m}$ from $i_{r,p,\mathrm{out},m}$ and $i_{r,f,m}$ from those calculation of the heat transfer.
2. Assume a value of R.
3. Calculation is performed from the first element to the last element, employing the following procedures:
   3.1 Assume an outlet moist air humidity ratio.
   3.2 Calculate the outlet moist air humidity ratio of each element by Eq. (31).
   3.3 If the outlet moist air humidity ratio obtained from step 3.2 is not equal to the assumed value of step 3.1, the calculation steps 3.1–3.2 will be repeated.
4. If the average of the individual outlet moist air humidity ratio for all elements of the last row is not equal to the total outlet moist air humidity ratio, assume a new R value and the calculation step 3 will be repeated until the average of the outlet moist air humidity ratio of the last row is equal to the outlet moist air humidity ratio.

C. Chilton–Colburn j-Factor for Heat and Mass Transfer (j_h and j_m)

The heat and mass transfer characteristics for the wavy fin-and-tube heat exchangers from the experimentation will be presented in the forms of the nondimensionless groups:

$$j_h = \frac{h_{c,\mathrm{out}}}{G_{a,\max}C_{p,a}}Pr_{\mathrm{out}}^{2/3} \tag{33}$$

$$j_m = \frac{h_{d,\mathrm{out}}}{G_{a,\max}}Sc_{\mathrm{out}}^{2/3} \tag{34}$$

IV. Results and Discussion

The dimensionless parameters representing the heat and mass characteristics are in terms of j_h and j_m, respectively. For comparison purpose, the measured results are shown with conventional reduction method by the Threlkeld method [13], and are shown in Figs. 7a–7c. For the heat transfer characteristic seen in Fig. 7a, the original lumped approach agrees well with the present discretized approach (89.67% of j_h within ±20%). However, the j_h obtained by the Threlkeld method is higher than those obtained by the present method. This difference arises because the j_h obtained by this study is based on discretized approach, whereas the Threlkeld method is applicable for fully wet surface only. For the results of the mass transfer characteristic shown in Fig. 7b, a larger difference of the j_m between those obtained by the Threlkeld method and the present method is observed (76.03% of j_m within ±30%). This is because the original process line approach derived by Threlkeld is based on for the counterflow arrangements. For further comparison with the tube-by-tube method proposed by Pirompugd et al. [8], as shown in Figs. 8a–8c, the j_h and j_m for fully wet condition obtained by the

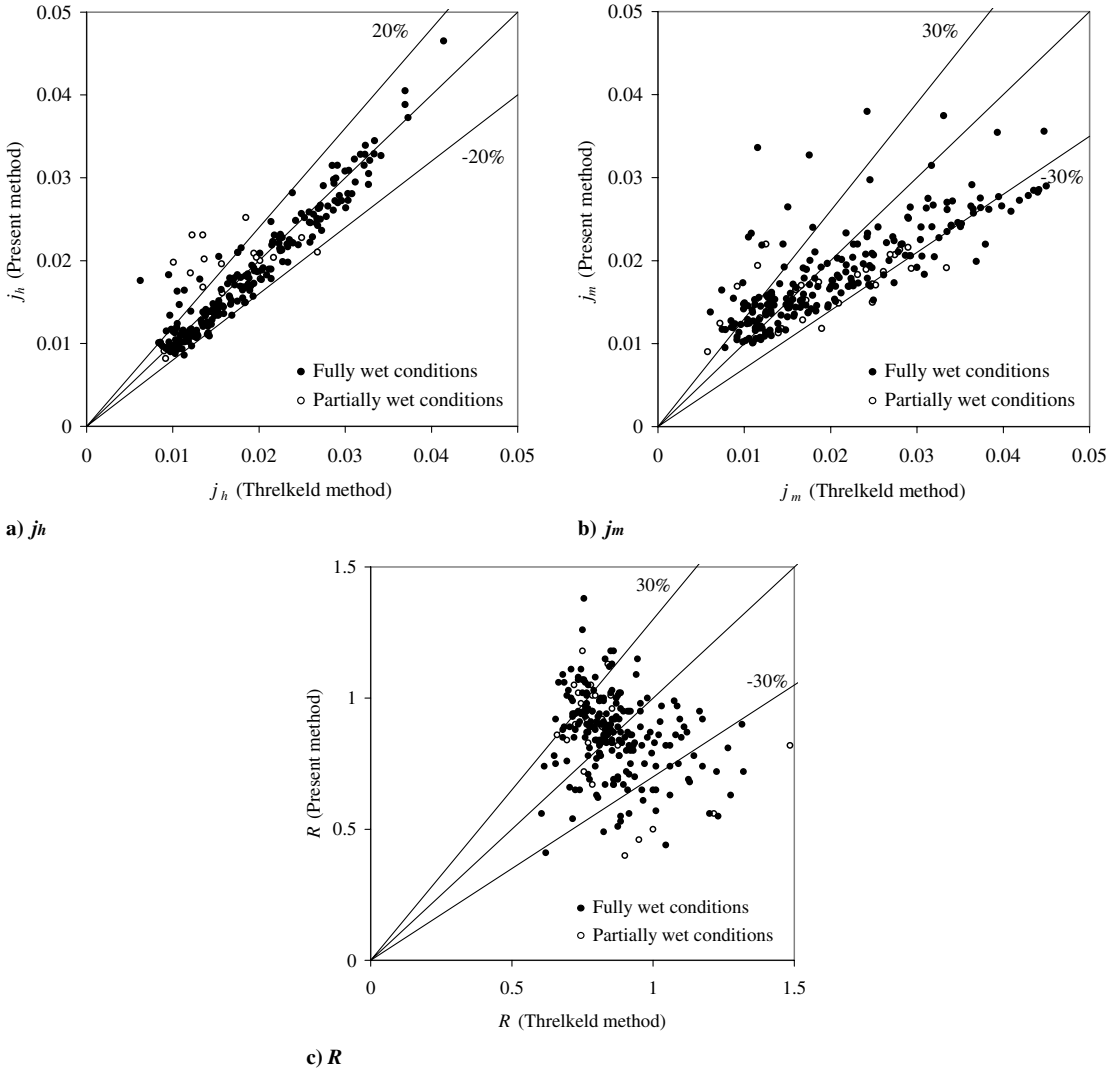

Fig. 7 Comparison between the data obtained from the present method and those obtained from the method of Threlkeld [13].

present method is equal to those obtained by the tube-by-tube method. However, for the partially wet conditions, a noticeable difference occurs for the j_h and j_m between those obtained by the present method and the tube-by-tube method. This is because the tube-by-tube method is suitable for fully wet condition, whereas the present method takes into account partially wet condition.

Influences of inlet relative humidity and of fin spacing in the heat transfer characteristics j_h are shown in Figs. 9a–9d. As seen in Figs. 9a–9d, when $1.18 \leq P_d \leq 1.68$, the effect of wave height on j_h is very small. These results agree well with those tested in dry conditions (Wang et al. [3,4,20]). Based on the simulation results in the published literatures (Ramadhyani [21] and Jang and Chen [22]), Wang et al. [20] pointed out that the j_h will be increased when the corrugation angle is larger than 20 deg. For the wet conditions, this discussion is still applicable to the results. When $N = 1$, one can see that j_h increases with decreasing fin spacing ($1.48 \leq S_p \leq 3.51$); however, it is insensitive to the inlet relative humidity. For $N \geq 2$, the j_h is insensitive to change of the inlet relative humidity and of fin spacing ($1.57 \leq S_p \leq 3.05$). For the influence of fin spacing on the heat transfer characteristic having $N = 1$ or $N = 2$, Wang and Chi [23] showed that their results are different from those in fully dry conditions. From the numerical simulation in the published literature (Torikoshi et al. [24]), they found when the fin spacing is small enough, the entire flow region can be kept laminar and steady and the vortex forms behind the tube can be suppressed. The increasing fin spacing would increase the cross-stream width of the vortex region behind the tube. Then, the j_h decreases with the increasing of fin spacing for one-row configuration, indicating a detectable influence of fin spacing. However, for the wet condition, negligible influence of fin spacing on the j_h is encountered. Apparently it is related to the presence of condensate, because it provides a good airflow mixing even at larger fin spacing. In fact, the difference in j_h can be negligible when the number of tube rows is increased. With the increasing number of tube rows, the subsequent row can block the condensate blowoff phenomenon from the preceding row.

The effects of inlet relative humidity and fin spacing on the j_m are shown in Figs. 10a–10d. When the fin spacing is sufficiently large (>2.0 mm), the influence of inlet relative humidity is relatively small. However, at smaller fin spacing, a slight decrease of j_m is observed when the inlet relative humidity is increased from 50 to 90%. The condensate retention phenomenon can be regarded as the main cause for the slight decreasing j_m with inlet relative humidity at dense fin spacing. The experimental results by Yoshii et al. [25], who observed the flow pattern of the airflow across a tube bank, showed that the blockage of the tube row by the condensate retention might hinder the performance of the heat exchangers. As a result, it may hinder the performance of the heat exchanger and a slight drop in the j_m. However, a considerable increasing j_m is evident when $RH = 0.5$ and $Re_{D_c} > 1200$. This can be attributed to the blowoff condensate by flow inertia, thereby making more room for water vapor. The decrease of influences on the j_h and j_m with the increasing number of tubes can be made clear by Wang et al. [26], who studied the flow visualization using scaleup fin-and-tube heat exchangers. Their study shows that the incoming air hits the first row tube, and then it twists and swirls to the subsequent row. The vertical motion is apparently stronger near the first row. The strength of the swirled

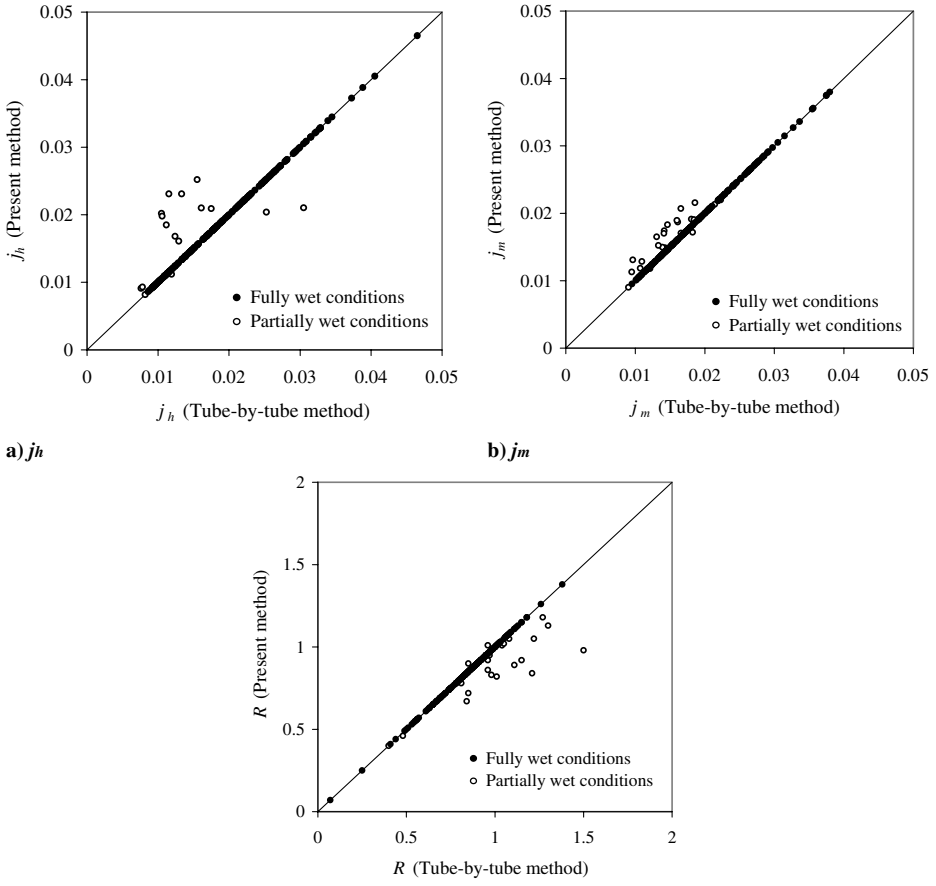

Fig. 8 Comparison between the data obtained from the present method and those obtained from the tube-by-tube method (Pirompugd et al. [8]).

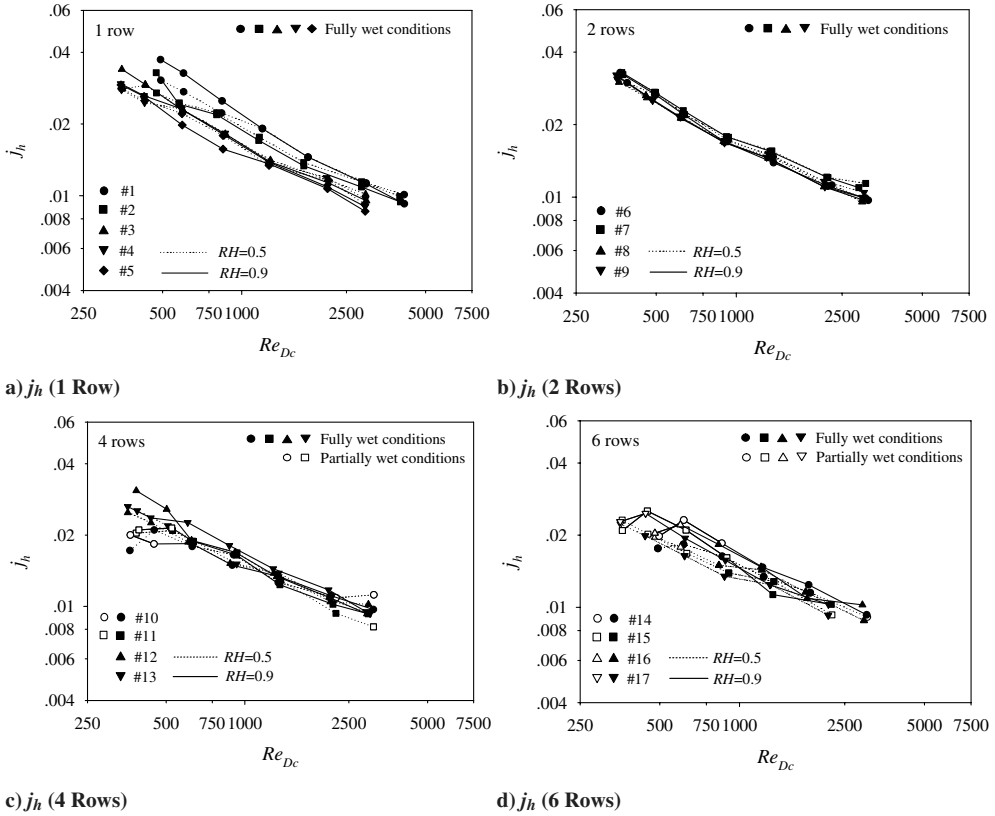

Fig. 9 j_h obtained from the present method.

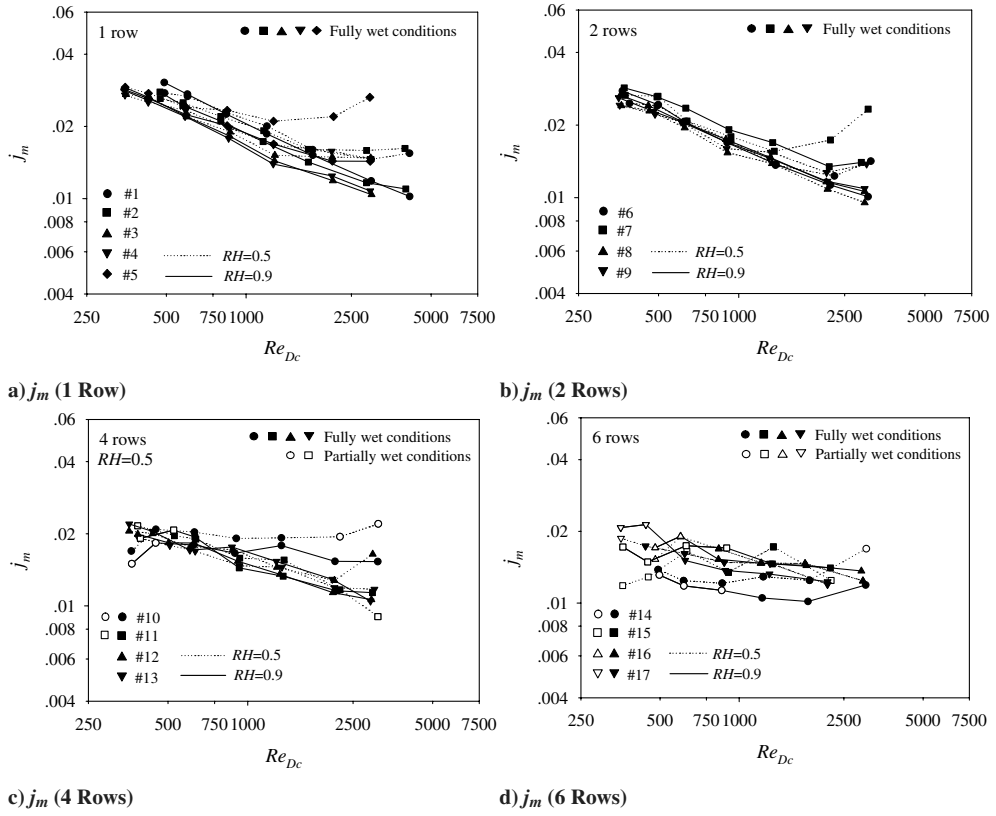

a) j_m (1 Row) b) j_m (2 Rows)

c) j_m (4 Rows) d) j_m (6 Rows)

Fig. 10 j_m obtained from the present method.

motion can be reduced by the increase of tube rows. In that regard, the influences of the geometry become insignificant with the number of tube rows.

For the simultaneous heat and mass transfer, if mass transfer data are unavailable, the analogy between the heat and mass transfer is convenient for reference. For an air–water vapor mixture, the ratio of $h_{c,o}/h_{d,o}C_{p,a}$ is about unity. The results of Seshimo et al. [27] and Eckels and Rabas [28] gave that this value is between 1.1 and 1.2. Hong and Webb [29] reported that this value is between 0.7 and 1.1. In this study, the values of $h_{c,o}/h_{d,o}C_{p,a}$ are between 0.6 and 1.2. However, the present authors found that the results from the Threlkeld method [13] did not entirely support the analogy between heat and mass transfer.

By using a multiple linear regression technique in a range of experimental data ($300 < Re_{D_c} < 5500$), the appropriate correlations of j_h and j_m based on the present data are as follows:

1) $N = 1$ (fully wet conditions)

$$j_{h,1,f} = 0.9998\left(\frac{S_p}{D_c}\right)^{0.5526}\varepsilon^{0.1912}Re_{D_c}^{(-0.4324\frac{S_p}{D_c}-0.0078\frac{P_l}{D_c}+0.0105\frac{P_t}{D_c}-0.431)} \tag{35}$$

$$j_{m,1,f} = 0.9996\left(\frac{S_p}{D_c}\right)^{1.8739}\varepsilon^{0.22}Re_{D_c}^{(-1.335\frac{S_p}{D_c}+0.058\frac{P_l}{D_c}+0.0407\frac{P_t}{D_c}-0.1487)} \tag{36}$$

$$R_{1,f} = 1.00\left(\frac{S_p}{D_c}\right)^{-1.38}\varepsilon^{-0.135}Re_{D_c}^{(0.8701\frac{S_p}{D_c}-0.0343\frac{P_l}{D_c}-0.0324\frac{P_t}{D_c}-0.3208)} \tag{37}$$

2) $N > 1$ (fully wet conditions)

$$j_{h,N,f} = j_{h,1,f}N^{-0.0718}\left(\frac{S_p}{D_c}\right)^{(-0.1114N-0.2044)}\varepsilon^{(-0.1478N+0.0539)} \times Re_{D_c}^{(0.0318N+0.3136\frac{S_p}{D_c}+0.0297\frac{P_l}{D_c}+0.0195\frac{P_t}{D_c}-0.2728)} \tag{38}$$

$$j_{m,N,f} = j_{m,1,f}N^{0.032}\left(\frac{S_p}{D_c}\right)^{(-0.2516N-0.3964)}\varepsilon^{(-0.3127N+0.3407)} \times Re_{D_c}^{(0.06722N+0.6516\frac{S_p}{D_c}+0.1775\frac{P_l}{D_c}-0.0721\frac{P_t}{D_c}-0.6235)} \tag{39}$$

$$R_{N,f} = R_{1,f}N^{0.0806}\left(\frac{S_p}{D_c}\right)^{(0.2053N+0.1357)}\varepsilon^{(0.1648N-0.2728)} \times Re_{D_c}^{(-0.0333N-0.3523\frac{S_p}{D_c}-0.1631\frac{P_l}{D_c}+0.0793\frac{P_t}{D_c}+0.4067)} \tag{40}$$

3) $N > 1$ (partially wet conditions) ($65\% < A_{\text{wet}}/A_{\text{tot}} < 100\%$)

$$j_{h,N,p} = j_{h,N,f}N^{-1.4809}\left(\frac{S_p}{D_c}\right)^{(-0.9515N+4.2239)}\left(\frac{A_{\text{wet}}}{A_{\text{tot}}}\right)^{(0.7134N-4.846)} \times Re_{D_c}^{(-0.1657N+0.9846\frac{S_p}{D_c}+0.2298\frac{P_l}{D_c}-0.176\frac{P_t}{D_c}+0.819)} \tag{41}$$

$$j_{m,N,p} = j_{m,N,f}N^{-1.3025}\left(\frac{S_p}{D_c}\right)^{(-0.73N+4.108)}\left(\frac{A_{\text{wet}}}{A_{\text{tot}}}\right)^{(1.1536N-7.9446)} \times Re_{D_c}^{(-0.1145N+0.445\frac{S_p}{D_c}+0.554\frac{P_l}{D_c}-0.4778\frac{P_t}{D_c}+0.9906)} \tag{42}$$

$$R_{N,p} = R_{N,f}N^{-1.0209}\left(\frac{S_p}{D_c}\right)^{(0.3N-2.67)}\left(\frac{A_{\text{wet}}}{A_{\text{tot}}}\right)^{(-0.8515N+4.673)} \times Re_{D_c}^{(0.0842N+0.6523\frac{S_p}{D_c}-0.39\frac{P_l}{D_c}+0.3349\frac{P_t}{D_c}-0.6755)} \tag{43}$$

Detailed comparisons of the proposed correlations against the experimental data are shown in Figs. 11a–11c. It is found that Eqs. (35), (38), and (41) can describe 99.18% of j_h within 20%, Eqs. (36), (39), and (42) can describe 86.89% of j_m within 20% and Eqs. (37), (40), and (43) can describe 88.93% of $h_{c,o}/h_{d,o}C_{p,a}$ within 20%.

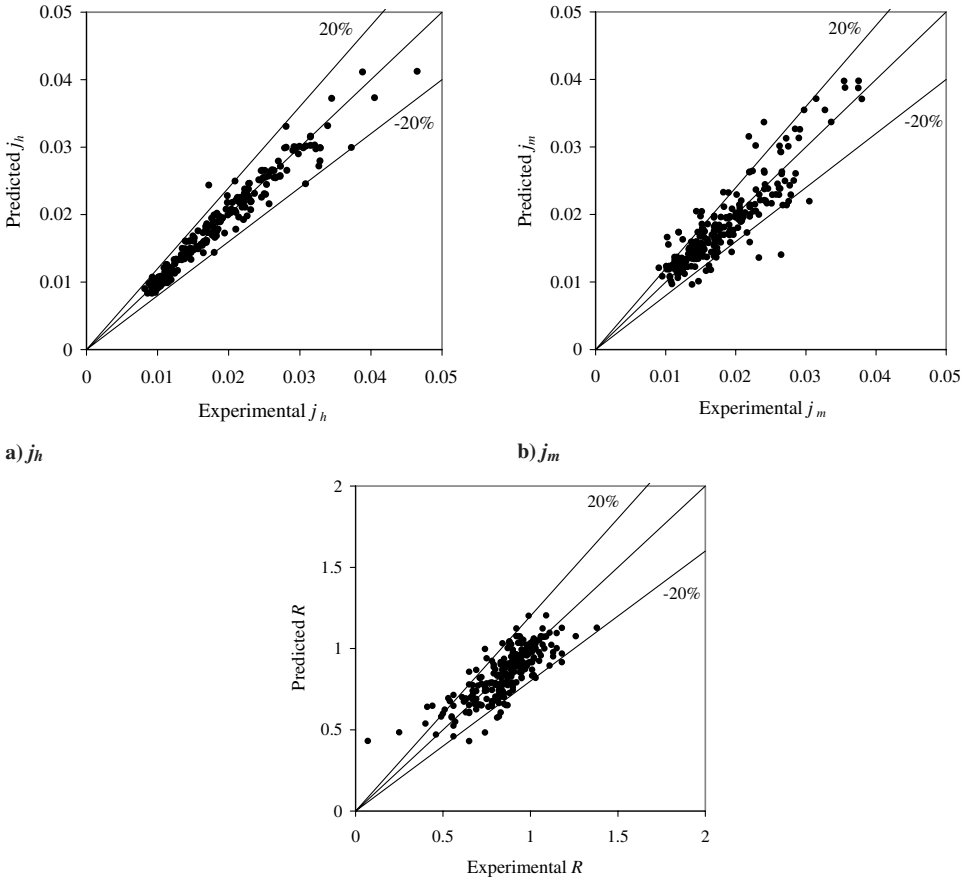

Fig. 11 Comparison between predicted data and experimental data.

V. Conclusions

This study proposes a new reduction method to analyze the heat and mass transfer characteristic of the experimental data from 17 wavy fin-and-tube heat exchangers under dehumidifying conditions. On the basis of the preceding discussions, the following conclusions are made:

1) A reduction method that is capable of handling fully wet and fully dry tiny circular fin method is proposed in this study. It is found that the proposed method is superior to previous method.

2) For fully wet conditions, the heat transfer and mass transfer characteristics obtained by the present method are relatively insensitive to the inlet relative humidity. However, the effect of relative humidity on the mass transfer characteristic becomes more pronounced when partially wet condition takes place.

3) The heat transfer characteristic is comparatively independent of the fin spacing. The effect of fin spacing on the mass transfer characteristic is rather small when fin spacing is larger than 2.0 mm. However, at a smaller fin spacing, j_m slightly decreases when the relative humidity increases.

4) The correlations are proposed for the present fin-and-tube heat exchanger having the wavy fin configuration. These correlations can describe 99.18% of j_h within $\pm 20\%$, can describe 86.89% of j_m within $\pm 20\%$, and can describe 88.93% of R within $\pm 20\%$.

Acknowledgments

The authors are indebted to the Thailand Research Fund (TRF) and the funding from Department of Industrial Technology of the Ministry of Economic Affairs, Taiwan for supporting this study.

References

[1] Beecher, D. T., and Fagan, T. J., "Effects of Fin Pattern on the Air-Side Heat Transfer Coefficient in Plate Finned-Tube Heat Exchanger," *ASHRAE Transactions*, Vol. 93, No. 2, 1987, pp. 1961–1984.

[2] Yan, W. M., and Sheen, P. J., "Heat Transfer and Friction Characteristics of Fin-and-Tube Heat Exchangers," *International Journal of Heat and Mass Transfer*, Vol. 43, No. 9, 2000, pp. 1651–1659.

[3] Wang, C. C., Fu, W. L., and Chang, C. T., "Heat Transfer and Friction Characteristics of Typical Wavy Fin-and-Tube Heat Exchangers," *Experimental Thermal and Fluid Science*, Vol. 14, No. 2, 1997, pp. 174–186.

[4] Wang, C. C., Tsi, Y. M., and Lu, D. C., "Comprehensive Study of Convex-Louver and Wavy Fin-and-Tube Heat Exchangers," *Journal of Thermophysics and Heat Transfer*, Vol. 12, No. 3, 1998, pp. 423–430.

[5] Wang, C. C., Lin, Y. T., and Lee, C. J., "Investigation of Wavy Fin-and-Tube Heat Exchangers: A Contribution to Data Bank," *Experimental Heat Transfer*, Vol. 12, No. 1, 1999, pp. 73–89.

[6] Wang, C. C., Hwang, Y. M., and Lin, Y. T., "Empirical Correlations for Heat Transfer and Flow Friction Characteristics of Herringbone Wavy Fin-and-Tube Heat Exchangers," *International Journal of Refrigeration*, Vol. 25, No. 5, 2002, pp. 673–680.

[7] Lin, Y. T., Hwang, Y. M., and Wang, C. C., "Performance of the Herringbone Wavy Fin Under Dehumidifying Conditions," *International Journal of Heat and Mass Transfer*, Vol. 45, No. 25, 2002, pp. 5035–5044.

[8] Pirompugd, W., Wongwises, S., and Wang, C. C., "Simultaneous Heat and Mass Transfer Characteristics for Wavy Fin-and-Tube Heat Exchangers Under Dehumidifying Conditions," *International Journal of Heat and Mass Transfer*, Vol. 49, Nos. 1–2, 2006, pp. 132–143.

[9] "Standard Methods for Laboratory Air-Flow Measurement," American Society of Heating, Refrigerating and Air-Conditioning Engineers (ASHRAE), Inc. Standard 41.2, Atlanta, GA, 1987.

[10] "Standard Method for Temperature Measurement," American Society of Heating, Refrigerating and Air-Conditioning Engineers (ASHRAE), Inc. Standard 41.1, Atlanta, GA, 1986.

[11] "Method of Testing Forced Circulation Air Cooling and Air Heating Coils," American Society of Heating, Refrigerating and Air-Conditioning Engineers (ASHRAE), Inc., Standard 33, Atlanta, GA, 1978.

[12] Moffat, R. J., "Describing the Uncertainties in Experimental Results," *Experimental Thermal and Fluid Science*, Vol. 1, No. 1, 1988, pp. 3–17.
[13] Threlkeld, J. L., *Thermal Environmental Engineering*, Prentice–Hall, New York, 1970.
[14] Bump, T. R., "Average Temperatures in Simple Heat Exchangers," *Journal of Heat Transfer*, Vol. 85, No. 2, 1963, pp. 182–183.
[15] Gnielinski, V., "New Equation for Heat and Mass Transfer in Turbulent Pipe and Channel Flow," *International Chemical Engineering*, Vol. 16, No. 2, 1976, pp. 359–368.
[16] Kern, D. Q., and Kraus, A. D., *Extended Surface Heat Transfer*, McGraw–Hill, New York, 1972, pp. 102–106.
[17] Myers, R. J., "The Effect of Dehumidification on the Air-Side Heat Transfer Coefficient for a Finned-Tube Coil," M.S. Thesis, Univ. of Minnesota, Minneapolis, MN, 1967.
[18] Wang, C. C., Hsieh, Y. C., and Lin, Y. T., "Performance of Plate Finned Tube Heat Exchangers Under Dehumidifying Conditions," *Journal of Heat Transfer*, Vol. 119, No. 11, 1997, pp. 109–117.
[19] Kandlikar, S. G., "Thermal Design Theory for Compact Evaporators," *Compact Heat Exchangers—A Festschrift for A. L. London*, edited by R. K. Shah, A. D. Kraus, and D. Metzge, Hemisphere, New York, 1990, pp. 245–286.
[20] Wang, C. C., Jang, J. Y., and Chiou, N. F., "Effect of Waffle Height on the Air-Side Performance of Wavy Fin-and-Tube Heat Exchangers," *Heat Transfer Engineering*, Vol. 20, No. 3, 1999, pp. 45–56.
[21] Ramadhyani, S., "Numerical Prediction of Flow and Heat Transfer in Corrugated Ducts," ASME Paper, HTD Vol. 66, 1986, pp. 37–43.
[22] Jang, J. Y., and Chen, L. K., "Numerical Analysis of Heat Transfer and Fluid Flow in a Three-Dimensional Wavy-Fin and Tube Heat Exchanger," *International Journal of Heat and Mass Transfer*, Vol. 40, No. 16, 1997, pp. 3981–3990.
[23] Wang, C. C., and Chi, K. U., "Heat Transfer and Friction Characteristics of Plain Fin-and-Tube Heat Exchangers: Part 1: New Experimental Data," *International Journal of Heat and Mass Transfer*, Vol. 43, No. 15, 2000, pp. 2681–2691.
[24] Torikoshi, K., Xi, G., Nakazawa, Y., and Asano, H., "Flow and Heat Transfer Performance of a Plate-Fin and Tube Heat Exchanger (First Report: Effect of Fin Pitch)," *10th International Heat Transfer Conference*, Paper 9-HE-16, Taylor and Francis, Washington, DC, 1994, pp. 411–416.
[25] Yoshii, T., Yamamoto, M., and Otaki, M., "Effects of Dropwise Condensate on Wet Surface Heat Transfer of Air Cooling Coils," *Proceedings of the 13th International Congress of Refrigeration*, International Institute of Refrigeration, Paris, 1973, pp. 285–292.
[26] Wang, C. C., Lo, J., Lin, Y. T., and Wei, C. S., "Flow Visualization of Annular and Delta Winglet Vortex Generators in Fin-and-Tube Heat Exchanger Application," *International Journal of Heat and Mass Transfer*, Vol. 45, No. 18, 2002, pp. 3803–3815.
[27] Seshimo, Y., Ogawa, K., Marumoto, K., and Fujii, M., "Heat and Mass Transfer Performances on Plate Fin and Tube Heat Exchangers with Dehumidification," *Heat Transfer, Japanese Research*, Vol. 18, No. 5, 1988, pp. 79–94.
[28] Eckels, P. W., and Rabas, T. J., "Dehumidification on the Correlation of Wet and Dry Transport Process in Plate Finned-Tube Heat Exchangers," *Journal of Heat Transfer*, Vol. 109, No. 3, 1987, pp. 575–582.
[29] Hong, T. K., and Webb, R. L., "Calculation of Fin Efficiency for Wet and Dry Fins," *International Journal of HVAC&R Research*, Vol. 2, No. 1, 1996, pp. 27–41.